

Effect of temperature on the dynamics of energetic displacement cascades: A molecular dynamics study

Horngming Hsieh, T. Diaz de la Rubia,* and R. S. Averback

*Department of Materials Science and Engineering,
University of Illinois at Urbana-Champaign, Urbana, Illinois 61801*

R. Benedek

Materials Science Division, Argonne National Laboratory, Argonne, Illinois 60439

(Received 8 May 1989; revised manuscript received 25 August 1989)

Molecular dynamics simulations of 3-keV displacement cascades in Cu at temperatures of 0, 300, 500, and 700 K have been performed using the Gibson II potential. Most atomic displacements occur in the quasimolten core region that develops at $t \sim 0.5$ ps and persists for several ps. The size and lifetime of the molten regions increase with ambient temperature, which results in a fourfold increase in atomic mixing between 0 to 700 K and a decrease in defect production. The instantaneous diffusion coefficients in the cascade melt are in close agreement with those in the equilibrium liquid.

Molecular dynamics (MD) simulation is a powerful tool for studying the dynamics of atomic motion in displacement cascades,^{1,2} and in particular the characteristics of thermal spikes.³⁻⁶ Recent simulations of cascades at 0 K have helped elucidate the role of thermal spikes in Cu and Ni.^{7,8} An important feature of those simulations was the indication of transient local melting in the cascade core, with the prominence of local melting being greater in Cu than in Ni. The primary evidence for melting in these studies^{7,8} was the similarity of the local pair distribution function in the central region of the cascade and the pair distribution function in the equilibrium liquid. Of course, this does not prove that precise local equilibrium is achieved, but it does suggest that a liquid-drop model represents at least the qualitative features of the process. A local temperature can always be defined operationally by equating the mean kinetic energy in a local region with $(3/2)kT$. Whether such an identification is useful depends on how similar the system behaves to a hypothetical locally equilibrated system with the same temperature profile $T(r)$. Several parameters could be monitored to test for local equilibration; in the present work we have analyzed the self-diffusion induced by displacement cascades generated at a series of ambient temperatures. By varying the ambient temperature of the lattice, the cooling rate and size of the cascade is altered. We will show that to a good approximation the diffusion coefficient is a function of local temperature, independent of the ambient temperature.

This study of the effect of temperature on ion beam mixing is also of interest for understanding radiation-enhanced diffusion (RED). Generally it is assumed that ion beam mixing and defect production are independent of temperature when solving the appropriate chemical rate equations for RED. However, it has not been possible to test this assumption experimentally due to the rapid motion of point defects after the cascade has cooled. The present fully dynamical simulations, which are the first to treat cascades above 0 K, thus provide the first semiquan-

titative estimates of the influence of temperature on ion beam mixing and defect production.

The MD code⁹ employed in this work closely followed the procedures of Gibson *et al.*¹⁰ In the 0-K simulations,⁷⁻⁹ two damped layers were employed inside a fixed boundary, with damping coefficients adjusted to mimic the flow of vibrational energy from the region of the computational cell to the surrounding medium. In the finite temperature studies, the damped layers are subjected to random forces, in accordance with Langevin dynamics,¹¹ which simulates contact with a heat bath. As in previous work,⁷⁻⁹ the computationally convenient Gibson II Cu Born-Mayer potential was employed; it is purely repulsive and has a cutoff between the first and second nearest-neighbor distances. The melting temperature for this potential is between 1000 and 1100 K.¹² 3-keV cascades were simulated by assigning the entire "knock-on" kinetic energy to an interior atom in the cell after equilibrating the crystal at 0, 300, 500, and 700 K. The 0 and 300 K events employed a lattice constant $a_0 = 3.608$ Å, and the higher-temperature lattice constants were dilated according to the observed thermal expansion coefficient of Cu, $\alpha = 1.7 \times 10^{-5}$. (Simulations for the Gibson II potential with Rahman-Parrinello boundary conditions yielded¹² $\alpha = 2.5 \times 10^{-5}$, in reasonable agreement with experiment.) The computational cell size, $23a_0$ on a side with 45 562 movable atoms, was sufficiently large that all displacements were contained in the cell and no substantial pressure buildup due to the fixed boundaries occurs.

In Fig. 1 are plotted the effective temperature versus time at the "center" of the simulated 3-keV cascades. This temperature is defined by averaging kinetic energy inside a sphere of radius $3.5a$ (~ 200 atoms); results are relatively insensitive to the exact sphere size. The center of the sphere is taken (somewhat arbitrarily) as the center of mass of the distribution of interstitial atoms created by the cascade event. Temperature is probably not meaningful for the first few tenths of picoseconds of the cascade. At $t \sim 0.5$ ps, however, the effective temperature is of the

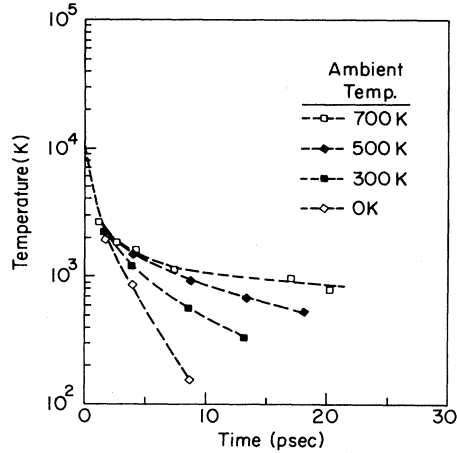


FIG. 1. Temperature in the center of a 3-keV cascade vs time. Events at four ambient temperatures are shown.

order of the (liquid-vapor) critical temperature [~ 6000 K (Ref. 13)], and considerable equilibration has occurred.

We have also monitored the atomic density in the central region as a function of time during the simulations.⁸ Although the density in this region is found to be lower than that of the matrix, it is still a few percent greater than the zero-pressure equilibrium values for the liquid at the corresponding temperatures shown in Fig. 1. In the 300-K cascade, for example, the atomic density at $t = 1.59$ ps when $T \sim 2200$ K is reduced by only -9.4% (relative to the equilibrium solid at 300 K) and by -5.5% at $t = 3.9$ ps, corresponding to $T \sim 1200$ K. For comparison, the (simulated) zero-pressure equilibrium volume of the liquid at the melting temperature is approximately 10% lower than that of the solid at 300 K. Thus, the locally melted region is effectively under compression. We ignore this complication in the discussion below, since it does not affect the qualitative behavior.

The time dependence of cascade temperature (cf. Fig. 1) can be fitted reasonably well by the form $[T(t) - T_0] \sim t^{-1.35}$, where T_0 is the ambient lattice temperature. This behavior corresponds rather closely to analytical thermal spike models:^{3,5} Seitz and Koehler,³ for example, find an exponent of -1.5 , based on the assumption of a temperature-independent thermal diffusivity.

To test the usefulness of temperature in characterizing the instantaneous state of a cascade, we have evaluated effective self-diffusion coefficients in simulated events as a function of time, using the relation

$$D(t) = (1/6N) \sum_i [\mathbf{r}_i(t + \Delta t) - \mathbf{r}_i(t)]^2 / \Delta t. \quad (1)$$

The sampled region is the same as that used in the temperature determination discussed above, and the time intervals Δt are of the order of 2 ps (cf. Fig. 1). Results for the simulated cascades at four ambient temperatures are plotted in Fig. 2 as a function of reduced cascade temperature, T/T_m , where $T_m = 1000$ K. Since the temperature varies continuously during the time interval Δt , the plotted temperature is the mean of the temperature at t and at

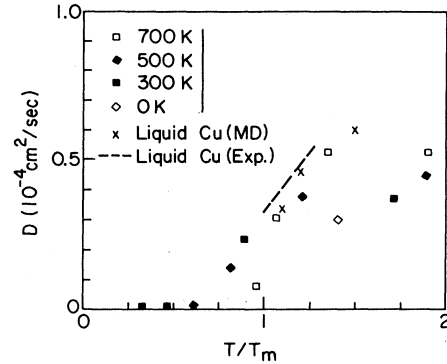


FIG. 2. Self-diffusion coefficients in the center of a 3-keV cascade plotted vs reduced temperature, T/T_m . Also shown (dashed line) are experimental Au tracer diffusion coefficients in liquid Cu (Ref. 14) and simulated values of self-diffusion in liquid Cu (Ref. 12).

$t + \Delta t$. Simulated equilibrium liquid Cu self-diffusion coefficients¹² for the Gibson II potential are shown for comparison, along with experimental values for Au tracer impurity diffusion in liquid Cu.¹⁴ The cascade diffusion coefficients in the reduced-temperature range 1 to 1.2 agree closely with liquid-state diffusion coefficients and confirm the local-melt interpretation of the cascade thermal spike.

The results for $T/T_m > 1.5$ most likely correspond to systems insufficiently equilibrated to give the correct liquid diffusion coefficients at those temperatures. We note also that the temperature variation for the 0-K cascade is probably too rapid for a meaningful diffusion coefficient to be obtained, although its magnitude is still similar to that in the liquid. After resolidification occurs ($T < T_m$), the diffusion coefficient is drastically reduced. In fact, the nonzero values obtained for D below T_m are most likely due to that part of the time interval, Δt , before resolidification is complete.

It is also instructive to consider the total amount of mixing,

$$\langle R^2(t) \rangle = \sum_i [\mathbf{r}_i(t) - \mathbf{r}_i(0)]^2, \quad (2)$$

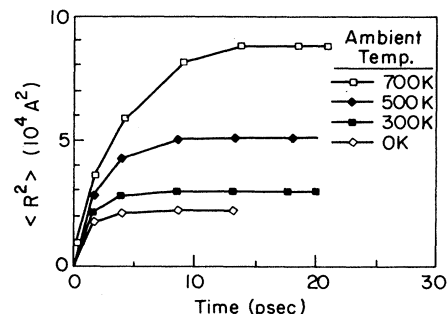


FIG. 3. Total atomic mixing in simulated 3-keV cascades as a function of time. Cascades at four ambient temperatures are shown.

which is plotted in Fig. 3. Here, the sum is over all atoms in the cell, although nearly all of the mixing results from those in the cascade core. $\langle R^2(t) \rangle$ increases rapidly at short times and saturates as the cascade region comes to equilibrium with the surrounding crystal (thermal diffusion of the vacancies and interstitials occurs on a longer time scale). By comparing the results in Fig. 3 with those in Fig. 1, we see that $\langle R^2(t) \rangle$ reaches its asymptotic value when T crosses T_m . This indicates that mixing virtually ceases when resolidification is complete.

We note that the total atomic mixing is a factor of 4 greater at 700 K ($\approx 0.7T_m$) than at 0 K. This behavior follows from the longer lifetime of the local melt, i.e., the time interval over which $T > T_m$ (cf. Fig. 1), and also from the larger size of the locally melted region in the higher temperature events. The maximum effective radius of the melt regions was $r_{\max} = (16, 20, 25, \text{ and } 29 \text{ \AA})$ for cascades at ambient temperatures $T = (0, 300, 500, 700 \text{ K})$. The temperature dependence of cascade-induced atomic mixing was previously discussed in Refs. 15 and 16, however, no reliable estimates of its magnitude exists. As mentioned above, ion-beam mixing is usually treated, for lack of a better procedure, as temperature independent in the analysis of ion-irradiation experiments at elevated temperatures, $T \approx 0.5T_m$, when RED dominates the mixing process. The experimentally observed differences between room-temperature and low-temperature values of mixing, however, are comparable to those found in our simulations.¹⁷ The temperature dependence of ion-beam mixing influences the kinetics of RED and concomitantly, the relative stability of different alloy phases under irradiation.¹⁸ The present results represent the first semirealistic estimates of this dependence from simulation.

Finally, we note that the number of Frenkel pairs produced in the simulated cascades at temperatures (0, 300, 500, 700 K) was (8, 3, 2, 3). With only a single event at

each temperature, it is not certain whether these numbers are characteristic, although a trend toward reduced defect production above 0 K is suggested by the results. The lower Frenkel pair production may result from shorter replacement sequences and larger droplet sizes; as discussed earlier,^{7,8} an interstitial must be transported beyond the melt boundaries to survive recombination during the thermal spike. Recombination resulting from interstitial migration at the elevated temperatures is also a possibility. It is noteworthy that the defect production efficiency at elevated temperatures found in these simulations relative to the Kinchin-Pease formula, i.e., $\approx 10\%$, is comparable to that deduced from macroscopic measurements of RED, radiation-induced segregation and radiation-induced embrittlement.¹⁹

In summary, cascade simulations at finite temperatures were performed for the first time. It was found that atomic mixing in cascade-induced thermal spikes in Cu can be accounted for primarily by quasi-liquid-state diffusion in a locally melted region. The mixing increases modestly with temperature up to 300 K and somewhat more rapidly at higher temperatures. Defect production, on the other hand, appears to decrease at elevated temperatures.

A helpful conversation with Roger Kelly is gratefully acknowledged. This work was supported by the U.S. Department of Energy, Basic Energy Sciences, under Grants No. DE-AC02-76ER01198 and No. W-31-109-ENG-38 at the University of Illinois and Argonne National Laboratory, respectively. The simulations were performed on the CRAY-2 at the Magnetic Fusion Energy Computer Center, Lawrence Livermore National Laboratory, under sponsorship of the U.S. Department of Energy, Basic Energy Sciences, and on the CRAY X-MP at the National Center for Supercomputing Applications at the University of Illinois.

*Present address: Lawrence Livermore National Laboratory, Livermore, CA 94550.

¹V. M. Agranovich and V. V. Kirsanov, in *Physics of Radiation Effects in Crystals*, edited by R. A. Johnson and A. N. Orlov (Elsevier, New York, 1986), p. 117.

²H. H. Andersen, Nucl. Instrum. Methods B **18**, 321 (1987).

³F. Seitz and J. S. Koehler, *Solid State Physics*, edited by F. Seitz and D. Turnbull (Academic, New York, 1956), Vol. 2, p. 307.

⁴P. Sigmund, Appl. Phys. Lett. **25**, 169 (1974); **27**, 52 (1975); P. Sigmund and M. Szymonski, Appl. Phys. A **33**, 141 (1984).

⁵G. H. Vineyard, Radiat. Eff. **29**, 245 (1976).

⁶R. Kelly, Radiat. Eff. **32**, 91 (1977).

⁷T. Diaz de la Rubia, R. S. Averback, R. Benedek, and W. E. King, Phys. Rev. Lett. **59**, 1930 (1987); *ibid.* **60**, 76(E) (1988).

⁸T. Diaz de la Rubia, R. S. Averback, R. Benedek, and H. Hsieh, J. Mater. Res. **4**, 579 (1989).

⁹A brief summary of the simulation model is given in W. E.

King and R. Benedek, J. Nucl. Mater. **117**, 26 (1983); the code was developed originally by J. R. Beeler, Jr.

¹⁰J. B. Gibson, A. N. Goland, M. Milgram, and G. H. Vineyard, Phys. Rev. **120**, 1229 (1960).

¹¹See, e.g., R. Biswas and D. R. Hamann, Phys. Rev. B **34**, 895 (1986).

¹²H. Hsieh (unpublished).

¹³M. M. Martynyuk, Russ. J. Phys. Chem. **57**, 195 (1983).

¹⁴A. Bruson and M. Gerl, Phys. Rev. B **19**, 6123 (1979).

¹⁵U. Shreter, F. C. T. So, B. M. Paine, and M-A. Nicolet, in *Ion Implantation and Ion Beam Processing of Materials*, edited by G. K. Hubler, O. W. Holland, C. R. Clayton, and C. W. White (North-Holland, New York, 1984), p. 31.

¹⁶D. Peak and R. S. Averback, Nucl. Instrum. Methods B **7/8**, 561 (1985).

¹⁷B. M. Paine and R. S. Averback, Nucl. Instrum. Methods B **7/8**, 666 (1985).

¹⁸G. Martin, Phys. Rev. B **30**, 1424 (1984).

¹⁹H. Wiedersich, Radiat. Eff. (to be published).